NUMERICAL ANALYSES ON THE SAFETY ASPECTS OF KASOLA TEST FACILITY

H. V. Hristov*, **T. Hollands**

Gesellschaft für Anlagen- und Reaktorsicherheit (GRS) gGmbH
Forschungszentrum Boltzmannstraße 14, 85748 Garching bei München, GERMANY
hristo.hristov@grs.de; thorsten.hollands@grs.de

M. Haselbauer, W. Jäger, W. Hering

Institute for Neutron Physics and Reactor Technology (INR)
Karlsruhe Institute of Technology
Hermann-von-Helmholtz-Platz 1, 76344 Eggenstein-Leopoldshafen, GERMANY
maxime.haselbauer@kit.edu; wadim.jaeger@kit.edu; wolfgang.hering@kit.edu

ABSTRACT

Sodium has been considered as main coolant candidate for Generation IV nuclear reactors. Due to its high chemical reactivity it however possesses hazardous potential. Extensive theoretical and experimental studies can deliver insights on the sodium handling and lead to improvements of the plants safety.

The Karlsruhe Sodium Laboratory (KASOLA) is an experimental research facility constructed around a sodium circuit. It is designated for research activities on thermal-hydraulics in sodium operated systems and supporting heat transfer studies for development and validation of turbulent heat transfer models for system and CFD codes.

The current work is focused on the investigation of the emergency drainage process of the KASOLA facility. As a first step, analyses of natural circulation occurring after pump trip and continuing operation of the air cooler and the test section heater have been carried out with ATHLET and ASTEC-Na system codes. Consequently, couple of drainage scenarios were defined and numerically examined. Those include normal and emergency drainage through the main drainage line. Failure of the valves on the air cooler evacuation lines was also investigated to establish the Na residual within the main circuit in that case. Further, two leak scenarios were postulated and theoretically analyzed with ATHLET in order to access the safety aspects of the facility. Response drainage procedures for different accident scenarios can be developed on the bases of the obtained results.

1. INTRODUCTION

The technologies based on the liquid metals as coolant are among the six reactor concepts, which are believed to represent the future shape of nuclear energy [1]. The Sodium Fast Reactor (SFR) is considered as main candidate for the forthcoming nuclear power plants. It can be used for both energy production and transmutation elements incineration – a way for closing the nuclear fuel cycle [2]. Using sodium in solar energy systems has recently also received increased interest [3]. Additionally, high temperature storage

---

* Corresponding author

capabilities of sodium operated facilities have attracted attention too since those are expected to exceed the storage temperature of the ones run with conventional medium such as water or oils [4].

Sodium has been preferred among the liquid metals due to its thermo-physical properties allowing broad temperature operational range at low pressure. These include large thermal conductivity, specific heat capacity and low density. Consequently, important safety features of SFR include long thermal response time, a reasonable margin to coolant boiling and a primary system that functions at almost atmospheric pressure. Sodium however possesses hazardous potential due to its high chemical reactivity. It reacts vigorously with the oxygen in the air and particularly violently with water. These chemical reactions are exothermic and the released by them heat can cause fire and endanger the safety of the sodium facility or plant.

KASOLA (KArlsruhe SOdium LAboratory) is a medium size experimental facility built at Karlsruhe Institute of Technology (KIT). It is planned to be used for research activities on the thermal-hydraulics of systems operating with sodium. The experiments can provide insights on the heat transfer in specific geometries as well as on components interactions. These can prove to be essential for the design and the optimization of all energy systems operating with sodium. Specifically in the case of SFR, its normal operation, transient behavior and emergency cooling devices can be investigated. The experiments can deliver valuable information on the turbulent heat transfer in liquid metals which is expected to lead to the development of heat transfer models for system and CFD codes [4]. It is also planned to use the facility for a feasibility study regarding the use of sodium as coolant and heat storage medium in a solar power plant [3, 5]. Further details on the KASOLA scientific program and on the planned experiments can be found in [6].

The drainage process of the base loop of the KASOLA test facility for several scenarios has been computationally analyzed in the current work. The drainage speed has been numerically predicted for different sodium temperatures and different initial coolant mass flows. Two break locations were postulated and theoretically analyzed to address the safety aspects of the facility. The numerical predictions can deliver the leaked sodium quantity for these accidents for different conditions. As a result, response procedures could be drawn on the bases of the numerical prediction to minimize the different accidents' impact.

2. KASOLA EXPERIMENTAL FACILITY

The KASOLA test facility (**Figure 1**) is located in the cylindrical steel building THINA of the Institute of Neutron physics and Reactor technology (INR) at the Karlsruhe Institute of Technology (KIT). During the seventies of the twentieth century an extensive experimental work on SFR has been carried out in THINA. The conducted research work has contributed to the development of enhanced know-how on the safety handling of liquid sodium within KIT particularly with respect of minimizing the risk of sodium leakages and fires. The building has an inner diameter of 7.7 m and a height of about 12 m. It is constructed from 10 steel ring segments with a thickness of 6 mm which are supported by an external grid. Choosing steel instead of concrete as a construction material improves the safety of the building if sodium leakage occurs. In that case, the released liquid sodium would not react with the chemically bonded water of the concrete, which reduces the risk of fire.

The main part of the KASOLA experimental facility is the 37.7 m long base loop which is schematically represented in **Figure 2** (blue line). It has been made of DN100 size steel pipes. All pipes are vertical or inclined at minimum of 4°, which reduces the risk of having sticking frozen sodium slugs at the pipe's walls. The KASOLA pipe lines and components have trace heating which can compensate the heat loses and keep the sodium in liquefied state. The base loop contains a 6 m long versatile test section above the magneto hydrodynamic pump (MHD). The test section can be used for development and investigation of

targets, component tests and experiments which require high mass flow rates [6]. At present, the test section is a straight pipe with heaters which can be positioned at different elevations. In combined operation with the sodium-air heat exchanger a natural circulation flow studies can be performed. The sodium-air heat exchanger is U-tube type with a maximum designed power of 970 kW. The primary (sodium) side of the heat exchanger has a volume of about 340 l. The heat exchanger drainage line (dotted red line containing NA-VSR-06 valve in **Figure 2**) is made of DN25 size pipe. The sodium temperature in the facility can be maintained between 150° to 550° C. The MHD pump can deliver a maximum sodium flow rate of 36.7 kg/s, which is monitored by a magnetic flow meter. Argon at 1.5 bar pressure is used as a sealing atmosphere of the loop to prevent sodium-air contact (green line in **Figure 2**). The expansion tank at the top can engross sodium volume changes due to temperature transients. In contrast to the leak-before-break method in nuclear power plants, alternative leakage detection methods have been utilized. This is necessary since the base loop is at low pressure, which is typical for sodium operated facilities. Firstly, an electrical current trough the base loop and a wire, which is placed between the base loop and the trace heating aids identifying sodium leaks. This method ensures detection within 1 to 2 seconds. Additionally, breaks can be recognized from the changes of the sodium level in the expansion tank and visually from the video observation of the building. The sodium storage tank is located outside the THINA building. Further details on KASOLA components can be found in [4].
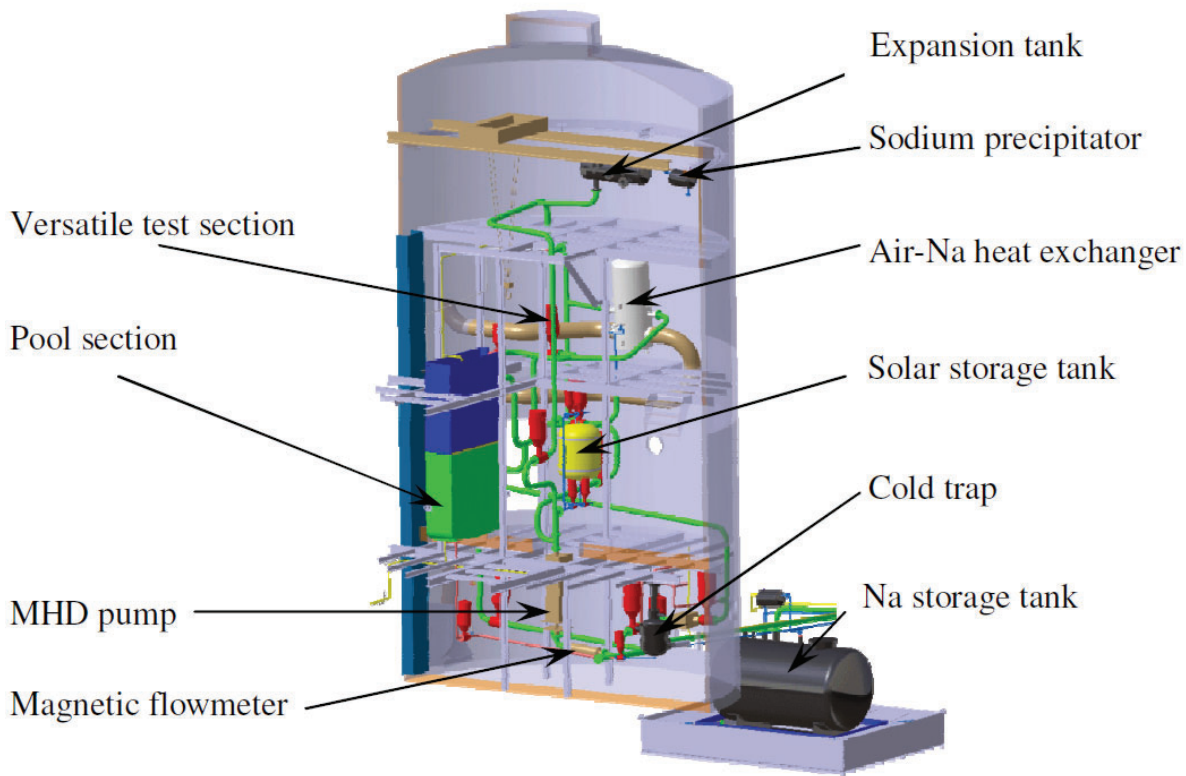

Figure 1. KASOLA test facility.

The KASOLA facility is controlled by two automatic Programmable Logic Controller (PLC) systems, one for general operation and one for the trace heating system [4]. In the case of power blackout, an emergency electricity supply will be activated for the PLC systems and the trace heating system. In the case of both PLC systems failure, an emergency heating system which is battery powered will be activated to ensure drainage of the sodium. All components can also be operated manually. The base loop

can be drained with the help of the MHD pump too, which can be switched in reverse pumping direction. To avoid thermal shocks in the sodium storage tank, the active drainage with the MHD pump is considered to be executed below 350 °C coolant temperature only. Gravity driven drainage will be performed in the case of sodium temperature above 350 °C. Further details on the KASOLA safety concept and the instrumentation of the facility are given in [4] and [5].
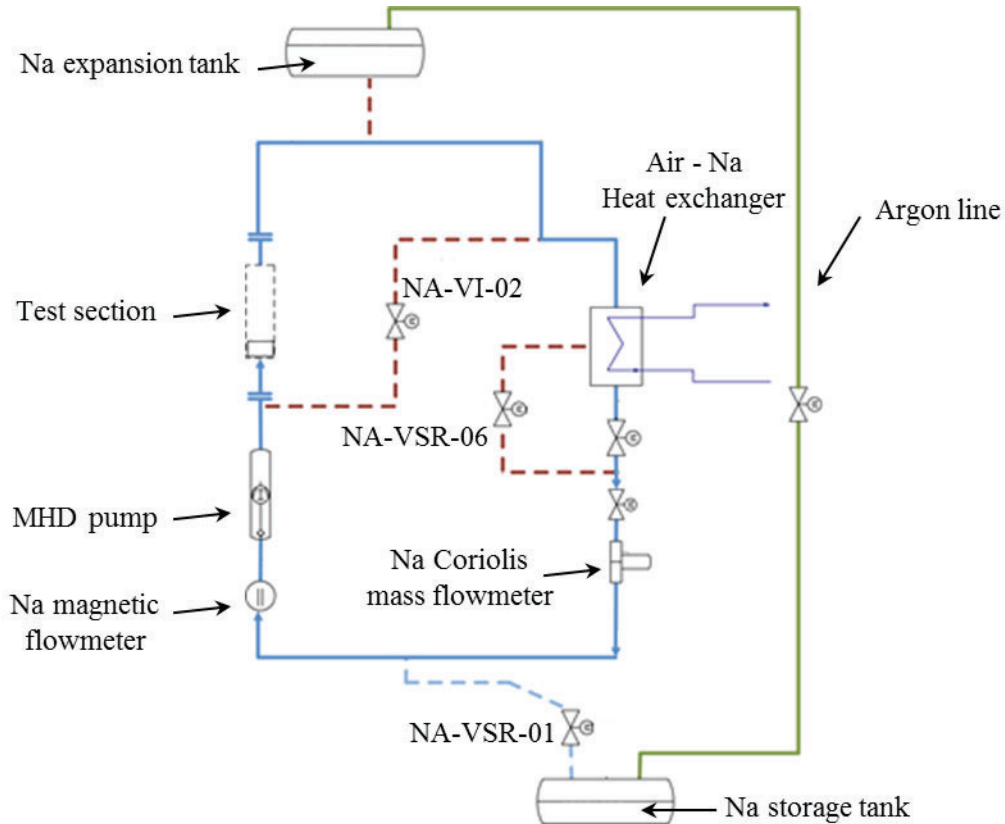

Figure 2. KASOLA base loop.

3. NUMERICAL MODEL OF THE EXPERIMENTAL FACILITY

A brief description of the ATHLET model for the KASOLA base loop is provided in this section. The ATHLET and ASTEC-Na models of the facility are in principle quite similar. Details on the ASTEC-Na model can be found in [7] and [8].

The ATHLET model (**Figure 3**) has been built in accordance to the schematic view of the KASOLA test facility depicted in **Figure 2**. The base loop incorporates two branches:
- Test section branch which includes the pipes NA-PI-01, NA-PI-02, NA-PI-03 and the part of NA-PI-04A up to the connecting point with NA-PI-13 line,
- Heat exchanger branch which includes the remaining part of NA-PI-04A, the heat exchanger NA-AHX-01, pipe NA-PI-04B, NA-PI-06 and NA-PI-07.

The two valves in the main loop (blue line in **Figure 2**) after the sodium-air heat exchanger remain open for all simulation scenarios and are represented by local flow resistance coefficients only. The same applies to the valve in the argon line connecting the expansion and the storage tanks. In both tanks the sodium level has been modeled with the level tracking model of ATHLET [9]. Special care has been taken with respect to the modeling of the expansion tank in order to correctly reproduce the sodium level-to-

volume ratio in the vessel. The storage tank has been represented by two cross-connected pipes. Such nodalization for the vessel can reproduce possible circulation flow. This, although currently not relevant, can indicate possible phenomena like thermal shock at the walls for future analyses. Even initial temperature distribution in the base loop i.e. same temperature for all components has been assumed for all simulation scenarios. The heat losses through the 100 mm pipe insulation have been presumed to be compensated by the pipe trace heating and the loop has been modeled as adiabatic.
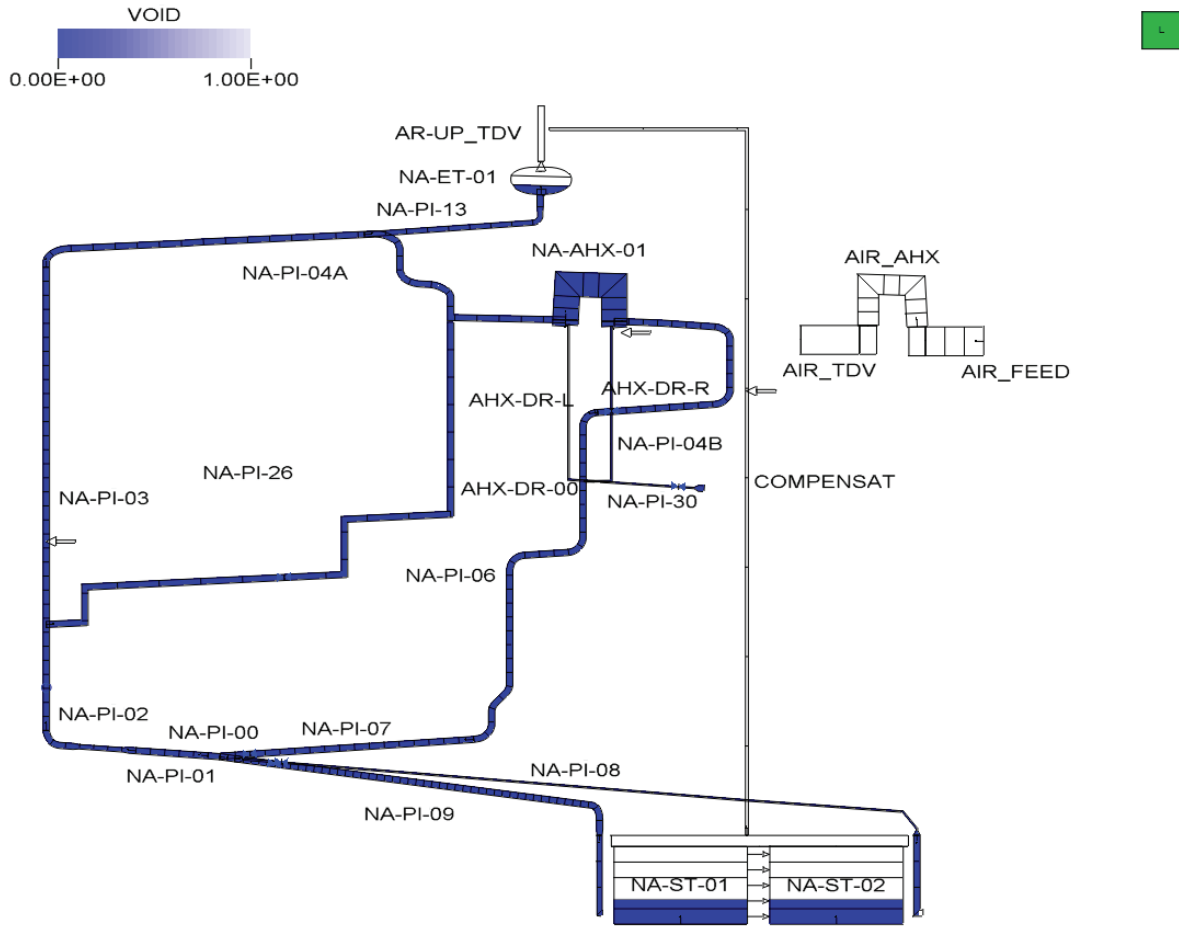

Figure 3. ATHLET nodalization scheme for KASOLA base loop.

The heat losses at the heated part of the test section have not been ignored for the natural circulation simulations. The counter-current sodium-air heat exchanger has been modeled with a single heat transfer structure with the geometrical parameters of the mean effective U-tube pipe. This single structure had a multiplier accounting for the total number of pipes in the heat exchanger. The air temperature and mass flow were provided accordingly in the case of natural circulation scenario. Otherwise, those were specified as zero for the air mass flow and as temperature equal to the one of the liquid sodium. The MHD pump has been modeled with the differential pressure pump model of ATHLET [9]. One second response time for the MHD pump has been assumed for both normal and reverse pumping directions. The pumping capacity has been calculated in the General Control Simulation Module (GCSM) module of ATHLET by multiplying the signal controlling the relative pump differential pressure by $f_d(\alpha_{Sodim,i-1} + \alpha_{Sodium,i})/2$. The f_d determines the pumping direction (positive or negative). It also sets the pump differential pressure to zero when the local argon volume fraction exceeds $\alpha_{Argon} = 0.7$. The exact pump head characteristic is unfortunately unknown and since the magnetic field can drive only the sodium, a simple liner proportionality term based on an averaged sodium volume fraction for the pump junction

$(\alpha_{Sodium,i-1} + \alpha_{Sodium,i})/2$ has been assumed. In the proportionality term, $i-1$ the represents the control volume in front of the MHD pump and i the one after it. The valves' characteristics and their response times were likewise unknown. The adopted, rather conservative valves' response time is summarized in **Table I**. Only the relevant for the simulations valves have been listed in **Table I**. The argon which is a standard gas option in ATHLET [9] has been modeled with its actual physical properties.

Table I. Valves' response times

Name	Response time, [s]
NA-VI-02	48
NA-VSR-01	20
Na-VSR-06	48

ATHLET (Analysis of THermal-hydraulics of LEaks and Transients code) is an advanced best-estimate code which has been initially developed for the simulation of design basis and beyond design basis accidents (without core degradation) in light water reactors, including VVER and RBMK reactors. The code has been extended to enable the simulation of further working fluids like helium and liquid metals. ATHLET contains two models: the 5-equations model with mean mixture momentum equation, and a two fluid 6-equations model. ATHLET uses the finite volume method. In the 5-equations models, the user can choose to deactivate the drift fluxmodel. Only the 5-equations model has been used for the current analyses.

CESAR is the thermal-hydraulics module of ASTEC-Na based on the finite volume approach [8]. It uses the two-fluid approach with a 5-equations model. Like in the case of ATHLET 5-equations model, an additional equation for the phase slip correlation can be inserted.

4. NATURAL CIRCULATION OF SODIUM

These simulations cases were carried out for preliminary code performance comparison. For the simulations, the air heat exchanger was operational and a heater at the lowest 2 meters of the test section was switched on. The wall heat losses for the heated part of the test section were calculated during the transient. At the heat exchanger inlet, the air had a temperature of 60 °C and a mass flow rate of 1.764 kg/s. All simulations started at nominal mass flow in the sodium circuit of 36 kg/s and temperature of 300 °C. The transition towards natural circulation flow was initialized by shutting down the MHD pump. Different simulation times were required by the different codes to achieve stable sodium mass flow in the KASOLA base loop. Both codes reached steady state flow conditions after about 8000 seconds problem time. The calculated sodium mass flow as a function of the heater power is presented in **Table II**. The difference between the predicted by the codes sodium mass flows is presented in the bottom row of the table.

Table II. Sodium mass flow rates at different heater power.

Heater power, [kW]		100	200	300	400	500	600
Na mass flow, [kg/s]	ASTAC-Na	1.545	1.985	2.301	2.555	2.770	2.954
	ATHLET	1.720	2.220	2.570	2.850	3.100	3.310
MF difference, [kg/s]		0.175	0.235	0.269	0.295	0.330	0.356

The maximum difference, observed at highest heater power (600 kW) is 0.356 kg/s, which roughly corresponds to 0.03 m/s sodium velocity. This discrepancy can be attributed to the slightly higher heat losses calculated with the ASTEC-Na model. Nevertheless, the code-to-code comparison for this case was considered satisfactory.

5. DRAINAGE OF KASOLA TEST FACILITY

Despite of the enhanced sodium-handling experience acquired during the years of research activities at KIT, the safety aspects have still to be addressed due to the hazardous potential of the coolant. In the case of accident or an undesired transient during an experiment, the sodium in the KASOLA loop has to be swiftly evacuated. Appropriate measures to minimize potential damages can be accordingly considered depending on the speed of drainage and possibly remaining liquid sodium in the base loop. Currently, information on the drainage process can be acquired from numerical simulations only. A preliminary study on the topic with an assumption of zero initial sodium mass flow has been previously performed [8]. The work has now been extended to include the following scenarios:

- Heat exchanger drainage valves operating normally with three subcases:
  - zero initial mass flow,
  - nominal initial mass flow,
  - drainage with active MHD pump,
- Malfunctioning of the heat exchanger drainage valves

5.1. Drainage of the KASOLA base loop with normally operating heat exchanger drainage valves

These simulations were performed for sodium temperature between 150 and 500 °C at about 50 °C thresholds. Heat losses through the pipes walls were ignored not only because of the good thermal insulation but also due to the presence of the trace pipe heating. The air heat exchanger was not considered to be operational during the drainage process.

The first case i.e. drainage at zero initial mass flow conditions had to be repeated due the difference in the valve opening time assumptions made in the preliminary study [8]. For the simulations with ASTEC-Na, valve opening times according to **Table I** were specified in [8]. ATHLET numerical predictions were not so conservative assuming valves' responding time of 2 seconds. In the current study, the initial and the boundary conditions for both codes were identically specified. The drainage initialization started with the opening of the NA-VSR-01 valve at the 10th second. The pump was coast down within one second in the case of nominal initial mass flow. For the active pump drainage scenario, the pump was modelled to reverse its pumping direction within two seconds. Hence, the pump pressure difference change from positive maximum to negative maximum within this time. The pump head was defined as a function of the local void as described in **Chapter 3**.

A comparison of ASTEC-Na and ATHLET predictions for the sodium mass flow in the drainage line NA-PI-09 in the case of zero initial coolant velocity is presented in **Figure 4 (a)**. The curves now appear quite close unlike the previous results [8]. This is on one hand due to the fact that the valves' response time was modelled the same but also due to the adopted valve characteristic in ATHLET model. The relative valve form loss coefficient is determined as a function of the CSA (Cross Section Area). For best numerical performance of the ATHLET valve model it is recommends to use the built-in table in which the relative flow loss coefficient increases exponentially for decreasing CSA. Such valves' characteristic is typical for fast responding valves. Having an opening time of 20/48 seconds makes the default option inappropriate. A quadratic dependency for the relative valve form loss coefficient was therefore provided as table in the ATHLET model. This produced the good match between the predictions of both codes as depicted in **Figure 4 (a)**. The predicted peak mass flow rate differs with about 1.5 kg/s. ASTEC-Na model calculates

the fastest drainage of the facility followed by the ATHLET predictions for which the interfacial drift flux model was switched off. The lower drainage speed predicted by ATHLET with an active interfacial drift flux model concern particularly the late stages of the process. This is caused by the indirectly increased interface friction, which becomes larger as the void rises and the flow enters annular flow regime. In annular flow regime the liquid phase flows like a film or droplets on the wall whereas the gas phase becomes the bulk one flowing at the center of the pipe or channel. It is not clear if such flow regime would at all occur when the KASOLA base loop is drained. It is also difficult to speculate on the predictions when more appropriate model is applied. It is however expected that when an accurate drift flux model is applied the results would be between the ones obtained with and without the drift flux model. It is obvious that model improvements and validation against experimental measurements is imperative.
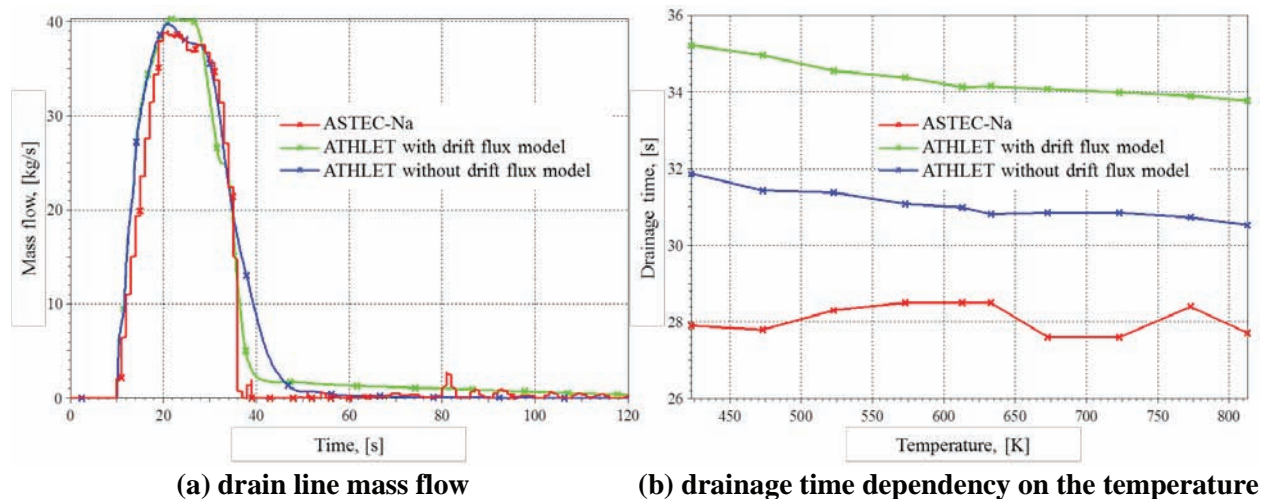

(a) drain line mass flow   (b) drainage time dependency on the temperature

Figure 4. Comparison of the numerical predictions of ATHLET and ASTEC-Na for the drainage of the KASOLA base loop.

The dependency of the drainage time on the temperature of the coolant is indicated in **Figure 4 (b)**. Both ASTEC-Na and ATHLET codes without active drift flux model predict drainage in the range of 30 seconds. The drainage time increases almost two fold by activating the drift flux model. In **Figure 4(b)** 30 seconds were deducted from the times predicted by ATHLET with drift flux model (green curve). Hence, by adding this 30 s to the green curve values in **Figure 4 (b)**, the calculated actual drainage times for the case can be obtained. This was done in order to be able to distinguish details in the predictions, which will be omitted at 26 to 66 seconds y axis. The drainage of the base loop is presumed completed when the sodium inventory within the circuit reduces below 95% of its initial amount. The same criterion has been already applied in the previous study [8]. The drainage speed is influenced by the dynamic viscosity and the density of the liquid sodium. The density decreases linearly with the temperature increase as shown in **Figure 5**. The sodium dynamic viscosity exhibits close to exponential dependency on the temperature (**Figure 5**). The natural logarithm of the viscosity is a combined rational and logarithmic function of the temperature. In **Figure 5** the highlighted in green region covers the operational temperature range of the KASOLA facility. For the entire region the density drop is about 1.07, whereas the viscosity one about 2.62. The driving force for the drainage of the facility is determined by the hydrostatic pressure, respectively the sodium density which will obviously decrease with the temperature rise by 1.07. The wall friction losses are proportional to the viscosity and the form losses are dependent on the density. Both decrease with the temperature rise. Hence, it is logical to expect that the system will drain faster at higher temperatures, which trend is also observed in **Figure 5** for ATHLET predictions. The ASTEC-Na prediction (red curve) in **Figure 4(b)** are scattered around 28 seconds and do

not show the expected dependency demonstrated by the ATHLET predictions. This can currently be attributed to the observed numerical instabilities of ASTEC-Na model. The calculated time difference between the times required for the drainage of the facility at the lowest (150 °C) and the highest (540°C) temperatures is only 1.02 second. This difference can however be significant for industrial facilities which operate with significantly larger sodium inventory.
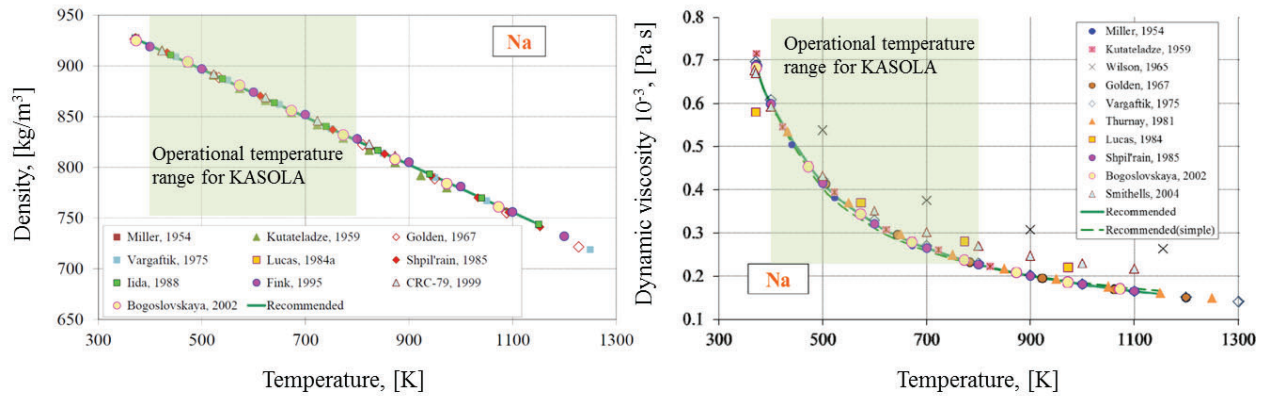

Figure 5. Sodium properties as a function of temperature [2].

The drainage of the base loop was also numerically investigated at nominal initial coolant flow rate with and without active pump as well. The nominal mass flow rate of about 36 kg/s in the base loop of the facility was achieved with activating the MHD pump with a positive relative differential pressure signal (**Figure 6 (b)**, up to the 10th second). In the case of drainage with an active MHD pump after the coast down, the pump differential pressure was directed in the opposite direction and made proportional to the local void fraction. As seen in **Figure 6 (b)**, the pump was working up to the 33rd second (23rd after drainage valve opening).

(a) drainage time of the base loop   **(b) relative pump differential pressure**
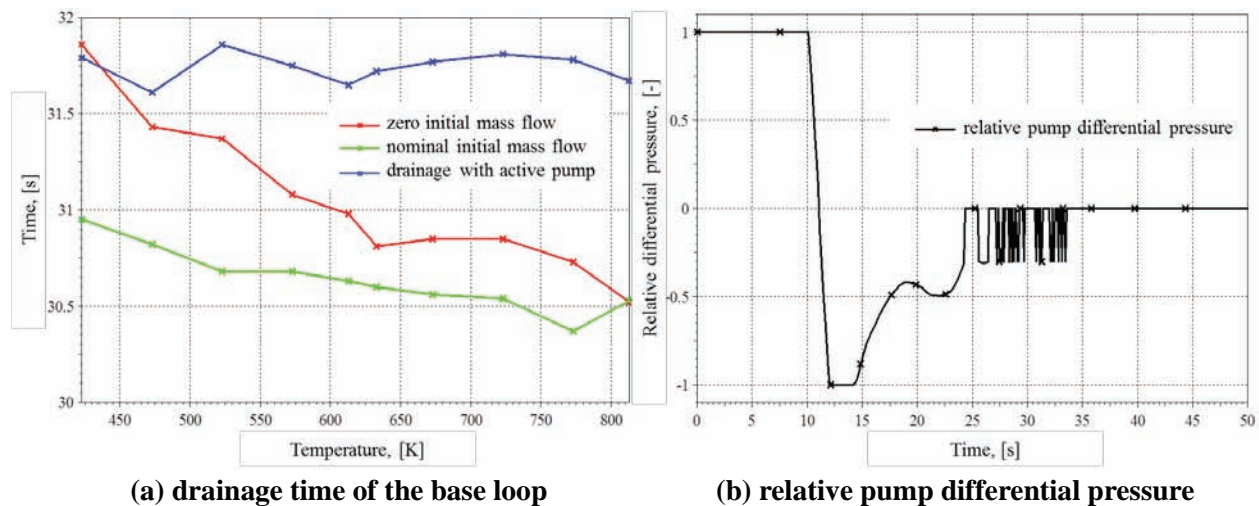
Figure 6. ATHLET prediction for the different drainage scenarios.

As indicated in **Figure 6 (a)**, the sodium will be evacuated most rapidly when the loop is at nominal initial mass flow. According to the numerical predictions, activating the pump in opposite direction actually slows down the drainage process by about a second (blue curve in **Figure 6 (a)**). This is a logical result since the pump in that case works also against the drainage of the heat exchanger branch of the main loop. This branch drains slower not only due to its bigger sodium inventory (found mainly within

the heat exchanger) but also due to its higher in comparison to the other branch local pressure losses (also previously shown [8]). The working in reversed direction pump increases the pressure at the bottom of the branch consequently reducing the drainage driving force for the heat exchanger branch. The demonstrated drainage time increase should not be taken for granted since the pump characteristic curve is at present not known. In that sense, the predicted results' trend can be affected by the applied simple pump model for the differential pressure. The presented in **Figure 6** drainage times were obtained with ATHLET with non-active drift flux model. However, similar behavior was calculated when this model was activated.

5.2. Malfunctioning of the heat exchanger drainage valves

The sodium mass in the AHX heat exchanger accounts for about one third of the of the total coolant mass in the base loop. Hence, in the case of AHX drainage valve malfunctioning (NA-VSR-06), it becomes important to establish the amount of sodium which would remain in the circuit. An additional accident scenario with quite elevated level of conservatism was further considered. For that, both the AHX drainage valve and the test section bypass valve (NA-VI-02) fail to open. Opening the NA-VI-02 valve would assist the drainage of the AHX heat exchanger due to the small inclination of the connecting part of pipe NA-PI-04A. The numerical predictions for both cases at 150 ° and 540 °C are summarized in **Table III**. The biggest part of the residual sodium is predicted to accumulate in the AHX heat exchanger when NA-VI-02 valve opens. However, when this valve also remains closed, the sodium inventory contained within in the test section bypass line surpasses the one in the heat exchanger.

Table III. Sodium inventory in the base loop in the case of heat exchanger drainage failure.

	Sodium mass						
	Total remaining in the base loop	% of the non-drained sodium	AHX and adjacent compo-nents	AHX heat exchanger	Drainage system of AHX	NA-PI-26	NA-PI-04A
	kg	%	kg	kg	kg	kg	kg
NA-VSR-06 closed NA-VI-02 closed							
150 °C	112.57	95.27	107.25	45.33	2.52	55.10	4.30
540 °C	100.00	95.92	95.92	39.97	2.41	50.00	3.54
NA-VSR-06 closed NA-VI-02 open							
150 °C	57.55	91.47	52.64	42.66	5.61	0.04	4.33
540 °C	50.32	91.18	45.88	39.86	2.42	0.04	3.56

6. LEAK SCENARIOS SIMULATIONS

The following two leak scenarios were postulated and numerically analyzed with ATHLET system code:
- break at beginning of the test section,
- break after the air heat exchanger.

The system has been modeled up to the break location. In that sense, no considerations have been made on the state of the sodium and its possible chemical reactions with the oxygen and the moisture of the THINA atmosphere past that location. The breaks were initialized at the 10th second of the transient simulation. For both cases a 10 cm^2 leak area was specified. The assumed size of the leak corresponds to

most severe rupture of a small instrumentation pipe, connected to the base loop. The local dimensionless pressure loss coefficient of the leak was 1.0. The temperature of the sodium in the circuit was 300 °C and the base loop was assumed to be at nominal coolant mass flow rate of 36 kg/s. Any heat losses through the walls of the pipes were ignored. In both cases the valve NA-VSR-01 and the heat exchanger drainage valves were opened with 1 second delay of the break initialization. The valves' response times were specified as given in **Table I**. Two cases were defined with respect to the test section bypass line valve NA-VI-02:

- closed NA-VI-02
- NA-VI-02 opens with the break initialization

Three pump modes(regimes) were postulated and their effect on the accident analyzed:

- reverse pump mode: reversed pumping direction initialized with the break opening
- pump coast down with the break initialization
- normal pump mode – pump control malfunctioning: the pump remains switched on in positive pumping direction for the entire simulation

For the first and the third pumping regimes, the pump head was corrected/reduced with the local void fraction (like in the case of the drainage simulations). The ambient temperature in the THINA building was 25 °C and the pressure was 1 atm. The response of the Argon sealing system was in addition considered. The following two cases were defined:
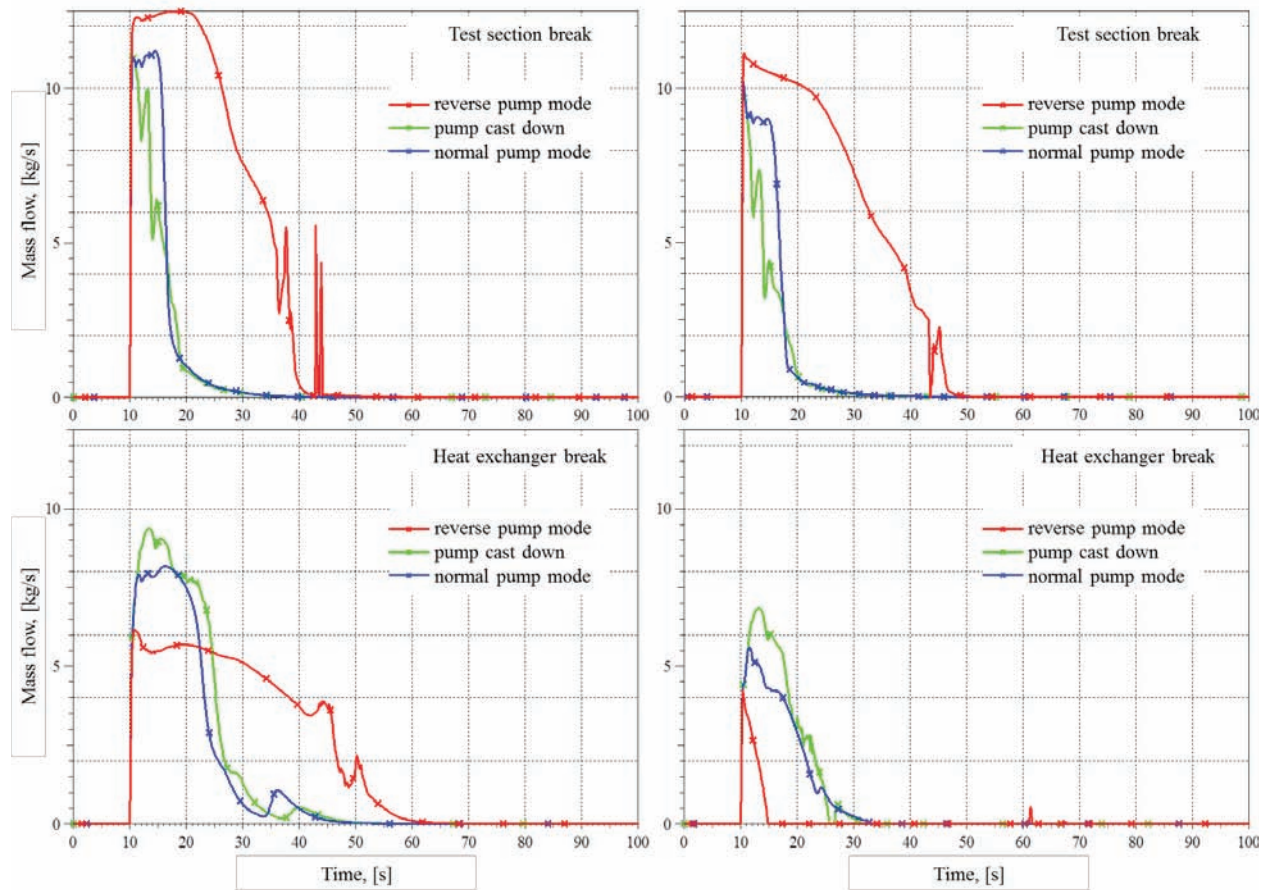
- Slow depressurization, for which the pressure difference between the KASOLA base loop and the THINA building levels due to the leak.
- Quick depressurization. For this case a connecting pipe between the COMPENSAT line (see **Figure 3**) and the volume representing the THINA building was built. A valve on this pipe opens with the break initialization. Since at that location at all times only argon is present, the pressure difference between the THINA building and the base loop diminishes quicker in comparison to the slow depressurization case.

The predicted leak mass flow rates in the case of slow and quick depressurization are shown in **Figure 7 (a)** and **(b)** respectively. The integral of the flow i.e. the total amounts of the leaked sodium to the KASOLA building are summarized in **Table IV**.

The highest leak mass flow rate of a 12.5 kg/s is predicted in the case of test section break at slow depressurization and active pump pumping in normal direction (red curve in **Figure 7 (a)** top). Quick depressurization helps reducing this mass flow by 1.5 kg at otherwise the same scenario conditions as indicated by the red curve in **Figure 7 (b)** top. Similar mass flow rate (11.0 kg/s) was calculated for the test section break with pump coast down – the blue curve in **Figure 7 (a)** top. However, in this case the leak mass flow quickly reduces between the 7th and the 8th second after initialization of the transient, which coincides with the reduction of the mass flow within the base loop after the pump has been switched off. Thereafter the leak mass flow depends on the hydrostatic pressure in the base loop at the leak location. This hydrostatic pressure decreases quicker in the case of test section break in comparison to the heat exchanger break as indicated by the blue curves in **Figure 7**. The test section branch is emptied quicker by both the leakage and drainage due to the lower pressure losses. This is reflected in the quicker pressure decrease. Only in the case of pump coast down, the hydrostatic pressure becomes dominant in determining the leak mass flow. Otherwise, the combination of the static and the dynamic pressures at the leak location controls the mass flow through the pipe rupture. Reversing the flow direction with the MHD pump reduces the leak mass flow in the case of test section break (also seen in **Table IV**). For the slow depressurization scenario the leaked sodium inventory is six times smaller in comparison to the case of pump operating in normal mode. Depressurizing the base loop quickly also helps reducing the amount of leaked sodium to the THINA building. By opening the test section bypass line valve NA-VI-02, the leakage mass is further slightly reduced in the case of test section break with a pump operating in reversed direction. This however, results from the fact that in the pump region the void increases slower due to the

flowing down sodium from the test section bypass line. Hence the pump can function for a bit longer according to the pump differential pressure model (**Chapter 3**).

The peak values for the leak mass flow in the case of the heat exchanger break are seen for the case of the pump operating in reverse direction (green curves in **Figure (a)** and **(b)** bottom). Those are lowered when the pump is coast down. The amount of the released sodium to the building is also reduced as seen in **Table IV**. Quick depressurization of the base loop reduces those integral values by half. At slow depressurization conditions and pump operating in normal direction, the break remains active for much longer time (red curve in **Figure 7 (a)**). Consequently, the highest amount at this break location of 190.12 kg and 211.22 kg (respectively open and closed NA-VI-02) is calculated (**Table IV**). The trends of the simulated leak mass flow rates in the case of quick depressurization are quite similar apart from the scenario with the pump operating in normal direction (**Figure 7 (a)** and **(b)** bottom). The ATHLET predictions for the last case (red curve in **Figure 7 (b)**) show that the leak mass flow will be significantly reduced if the pump remains active in that mode. According to **Table IV** this reduction, depending on the NA-VI-02 valve is about 17 to 19 times in comparison to the worst case with a pump working in reversed regime. It is also a fivefold improvement against the second-best case when the pump is coast down with the break initialization – 11.10 kg against 54.18 kg.

(a) slow depressurization of the base loop   (b) quick depressurization of the base loop

Figure 7. Leak mass flow rates (sodium).

The reduction of the leaked sodium amount results from the quick depressurization and from the effect of the pump. The pump in normal operation mode creates under pressure in the heat exchanger branch and decreases the drainage speed of the test section branch. Thus, it becomes easier to drain the sodium from the heat exchanger branch towards the storage tank. These contribute beneficially to minimize the leaked sodium mass and reduce it to very low values compare to the other simulations. According to **Table IV**, opening the valve in the test section bypass line worsens the severity of the accident (apart from the described above case for the test section break and pump in reversed mode). When NA-VI-02 opens, the tapped in the upper part of the bypass line about 55 kg of sodium can now freely flow and influence the leak mass flow. In the case of normal and reverse pump mode, this amount of sodium contributes to the local pump void causing longer pumping availability. If the pump is coast down, the sodium within the bypass line would contribute to the faster reduction of the flow speed in the base loop (NA-VI-02 open). The hydrostatic pressure in the test section branch will remain higher for longer time span in comparison to the cases when NA-VI-02 remains closed. As indicated in **Table IV**, the leaked sodium is now increased for all simulations with the maximum calculated value of 317.90 kg for test section break at normal pump mode. The influence is much smaller for the heat exchanger break scenarios.

Table IV. Sodium amount leaked to the KASOLA building.

Simulation case	Slow depressurization		Quick depressurization	
	Test section break	AHX heat exchanger break	Test section break	AHX heat exchanger break
	Total amount of leaked sodium, [kg]			
NA-VI-02 closed				
pump in reverse direction	62.97	135.97	48.64	66.69
non-active pump	78.07	116.99	66.87	54.18
pump in normal direction	280.15	190.12	262.13	11.10
NA-VI-02 open				
pump in reverse direction	61.20	147.22	47.72	68.46
non-active pump	89.57	117.68	83.07	54.92
pump in normal direction	317.90	211.22	288.27	11.71

7. CONCLUSIONS

Two main safety aspects of KASOLA test facility were computationally examined in the work:
- Drainage of the base loop at different initial conditions
- Postulated break scenarios

The drainage of the base loop is relevant for operational transients when a swift evacuation of the sodium can be desired. The second safety aspect is important in the case of accidents for which the possible consequences can be theoretically accessed.

According to the numerical analyses with ATHLET and ASTEC-Na, the sodium in base loop of the facility would drain within about 31 (28 calculated with ASTEC-Na) to 64 seconds. This 33 seconds time difference results from the lack or application of the drift flux model. In general, the application of the

drift flux model is necessary in order to correctly reproduce the momentum exchange between the gas and the liquid phases. The model has been successfully applied in the past to two-phase steam-water systems. It however has not been validated for flow gas and liquid metals interactions for which an extensive experimental data is required. Conducting drainage experiments of the KASOLA base loop would be of great contribution for the improvement of this model.

The ATHLET simulations for the break scenarios show that a quick depressurization of the KASOLA base loop would reduce the amount of leaked to the building sodium. A vital contribution along those lines can have the pump operating mode. It was shown that in the case of test section break, operating the MHD pump in a reverse mode would benefit the safety. On the contrary, leaving the pump in normal operation mode in the case of heat exchanger break can extremely reduce the amount of the leaked sodium. Hence, according to the presented ATHLET results, the released sodium amount in the KASOLA building can be controlled when an appropriate response procedure after the break onset is applied. Further theoretical investigations can aid finding an optimal response procedure for different postulated accident scenarios and enhance the safety of the KASOLA facility. Similar analyses can clearly contribute to the safety improvements of plants operating with liquefied sodium.

ACKNOWLEDGMENTS

REFERENCES

1. GIF (2002), "A Technology Roadmap for Generation IV Nuclear Energy Systems", GIF-002-00, USDOE Nuclear Energy Research Advisory Committee and the Generation IV International Forum, (2002)   .
2. V. Sobolev, "Database of thermophysical properties of liquid metal coolants for GEN-IV, Sodium, lead, lead-bismuth eutectic (and bismuth)", Scientific Report SCK•CEN-BLG-1069, Belgian Nuclear Research Centre, Belgium, (2010).
3. W. Hering, R. Stieglitz, T. Wetzel, "Application of liquid metals for solar energy systems", European Energy Conference, Maastricht, Netherlands, April 17-20, (2012).
4. A. Onea, W. Hering, C. Homann, A. Jianu, M. Lux, S. Scherrer and R. Stieglitz, "Optimisation of the KASOLA high temperature liquid metal loop", NURETH15-545, The 15th International Topical Meeting on Nuclear Reactor Thermal – Hydraulics, NURETH-15, Pisa, Italy, May 12-17, (2013).
5. W. Hering, S. Stieglitz, "Qualification requirements for innovative instrumentation in advance nuclear systems", Proc. Of the 8th PAMIR International Conference on Fundamental and Applied MHD, Corsica, France, (2011).
6. W. Hering, S. Stieglitz, A. Jianu, M. Lux, A. Onea, S. Scherrer, Ch. Homann, "Scientific program of the Karlsruhe Sodium Laboratory (KASOLA)", *IAEA-CN-199/257,* Int. Conf. on Fast Reactors and Related Fuel Cycles, Paris, France, March 4–7, (2013).
7. S. Perez-Martin, M. Haselbauer, W. Pfrang, W. Hering, "Contribution of KIT to the development of ASTEC-Na code Part I: Modeling of the KASOLA loop", Annual Meeting on Nuclear Technology – Jahrestagung Kerntechnik 2014, Frankfurt am Mein, Germany, May 6–8, (2014).
8. M. Haselbauer, W. Jäger, W. Hering, H. V. Hristov, T. Hollands, "Purge simulations on the KASOLA Sodium loop. Sensitivity study and code-to-code comparison", Proceedings of ICAPP 2015, Paper 15352, Nice, France, May 3-6, (2015).
9. G. Lerchl, H. Austregesilo, P. Schöffel, D. von der Cron, F. Weyermann, "ATHLET Mod 3.0 Cycle A User's Manual", GRS-P-1 / Vol. 1 Rev. 6, Garching bei München, Germany, (2012).